Geophysical Research Letters

RESEARCH LETTER
10.1029/2019GL086357

Quantifying Atmospheric Trace Element Deposition Over the Ocean on a Global Scale With Satellite Rainfall Products

David Kadko[1], William M. Landing[2], and Clifton S. Buck[3]

[1]Applied Research Center, Florida International University, Miami, FL, USA, [2]Department of Earth, Ocean and Atmospheric Science, Florida State University, Tallahassee, FL, USA, [3]Skidaway Institute of Oceanography, University of Georgia, Savannah, GA, USA

Key Points:
- Aerosol input of trace element micronutrients is difficult to determine as aerosol chemical concentration alone cannot yield deposition rate
- The natural radionuclide ^{7}Be provides a means to estimate the bulk deposition velocity (V_b) required to calculate aerosol fluxes
- We use new ^{7}Be data from the Pacific with data from other ocean basins to derive a global relationship between rain rate and V_b

Supporting Information:
- Supporting Information S1
- Table S1

Correspondence to:
D. Kadko,
dkadko@fiu.edu

Citation:
Kadko, D., Landing, W.M., & Buck, C.S. (2020). Quantifying atmospheric trace element deposition over the ocean on a global scale with satellite rainfall products. *Geophysical Research Letters*, *47*, e2019GL086357. https://doi.org/10.1029/2019GL086357

Received 22 NOV 2019
Accepted 12 MAR 2020

Abstract Atmospheric input of trace element micronutrients to the oceans is difficult to determine, as even with collection of high-quality aerosol chemical concentrations, such data by themselves cannot yield deposition rates. To transform these concentrations into rates, a method of determining flux by applying an appropriate deposition velocity is required. A recently developed method based on the natural radionuclide ^{7}Be has provided a means to estimate the bulk (wet + dry) deposition velocity (V_b) required for this calculation. Here, water column ^{7}Be inventories and aerosol ^{7}Be concentrations collected during the 2018 US GEOTRACES Pacific Meridional Transect are presented. We use these data together with those from other ocean basins to derive a global relationship between rain rate (m/yr) and bulk deposition velocity (m/day), such that $V_b = 999 \pm 96 \times \text{Rain rate} + 1{,}040 \pm 136$ ($R^2 = 0.81$). Thus, with satellite-derived rainfall estimates, a means to calculate aerosol bulk deposition velocities is provided.

Plain Language Summary Atmospheric input of trace element micronutrients to the global ocean such as iron (Fe), cobalt (Co), and Zinc (Zn) is difficult to determine. Even with collection of high-quality aerosol chemical concentrations, such data by themselves cannot yield rates of deposition. A recently developed method based on the natural radionuclide ^{7}Be, which is deposited to the surface ocean, has provided a means to estimate the bulk (wet + dry) deposition velocity (V_b) required for this calculation. In this work, water column ^{7}Be inventories and aerosol ^{7}Be concentrations collected during the 2018 US GEOTRACES Pacific Meridional Transect are presented. We use these data together with those from other ocean basins to derive a global relationship between rain rate (m/yr) and bulk deposition velocity (m/day), such that $V_b = 999 \times \text{Rain rate} + 1{,}040$ ($R^2 = 0.81$). Thus, deposition velocity to an ocean region can be estimated from rainfall rate. This information is critical for evaluating limitations on phytoplankton growth and the strength of the biological carbon pump and represents an important input to ocean biogeochemical models.

1. Introduction

As the base of most marine food webs, phytoplankton productivity affects growth and success at all other trophic levels in the oceans. Phytoplankton growth rates are controlled in part by macronutrient and micronutrient supply rates, which in turn are controlled by physical environmental factors (atmospheric deposition, vertical mixing, upwelling, and horizontal advection), which vary over (and often define) different oceanic regimes. The magnitude of these fluxes will therefore vary significantly across ocean basins (e.g., Buck et al., 2019; Kadko et al., 2020). The biological carbon pump, one of the dominant mechanisms for sequestering atmospheric carbon to the deep ocean (Volk & Hoffert, 1985), is related to the interplay between different limiting factors such as the concentrations of available macronutrients (silicon, Si; phosphorus, P; nitrogen, N) and essential micronutrients like manganese (Mn), iron (Fe), cobalt (Co), nickel (Ni), copper (Cu), zinc (Zn), and cadmium (Cd). Understanding the factors that control the sources and distributions of bioactive trace elements (TEs) is crucial for predicting their effects on the biological carbon pump.

Atmospheric input to the oceans can be significant for many chemical species (e.g., Duce et al., 1991; Prospero, 1996, 2002). TE micronutrients delivered to the open ocean by dust deposition may, in some areas, relieve TE limitation on phytoplankton growth and promote nitrogen fixation (e.g., Baker & Jickells, 2016; Coale et al., 1996; Falkowski, 1997; Falkowski et al., 1998; Jickells et al., 2014; Krishnamurthy et al., 2009;

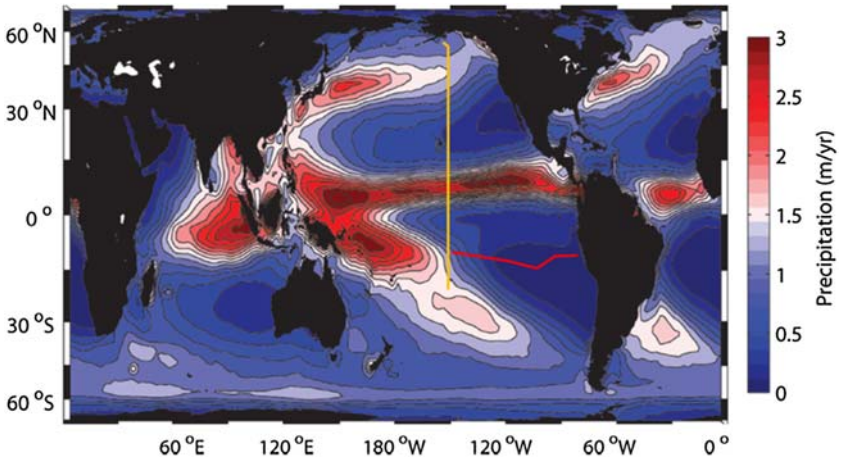

Figure 1. The track (yellow line) of the 2018 GEOTRACES PMT (GP15) cruise superimposed over a climatological map of precipitation from Schanze et al. (2010). Also shown is the track (red line) of the 2013 GEOTRACES GP16 (East Pacific Zonal transect; Kadko et al., 2020).

Martin et al., 1990; Moore et al., 2002, 2009, 2013; Okin et al., 2011) and can play an important role in controlling biogeochemical processes in the ocean (e.g., Morel et al., 2003; Morel & Price, 2003). For these reasons, considerable effort has been made to evaluate the supply of dust to the ocean (e.g., Anderson et al., 2016; Baker et al., 2016) including consideration of dust supply in global biogeochemical models (e.g., Mahowald et al., 2005; Tagliabue et al., 2009, 2015). Despite these efforts, the determination of the dust flux, particularly in remote ocean regions, is difficult (Anderson et al., 2016; Baker et al., 2016). While direct collection of atmospheric aerosols is relatively straightforward, there is limited availability of island sampling locations, and collection during a research cruise offers only a brief snapshot of aerosol loading. Furthermore, even with high-quality aerosol chemical concentrations obtained from shipboard or land-based aerosol samples, such concentration data by themselves cannot yield the deposition rate of TEs. To transform these concentrations into rates, a method of determining flux by applying an appropriate deposition velocity is required. Similarly, the parameterization of atmospheric deposition processes may be inaccurately configured (poorly constrained) in global-scale biogeochemical models. If such parameters could be accurately assessed, then the chemical concentrations in aerosol samples could be converted into actual estimates of flux.

A recently developed method based on the natural radionuclide ^{7}Be (half-life 53.3 days) has shown promise as a way to estimate atmospheric deposition fluxes (Kadko et al., 2015). This method has been used to derive TE atmospheric fluxes for sites in the Atlantic (Anderson et al., 2016; Kadko et al., 2015; Shelley et al., 2017), the Pacific (Buck et al., 2019; Kadko et al., 2020), and the Arctic (Kadko et al., 2016; Kadko et al., 2019; Marsay et al., 2018) Oceans. ^{7}Be is produced in the upper atmosphere from cosmic ray spallation, quickly attaches to aerosol particles, and is transported to the lower troposphere by atmospheric mixing processes and removed mainly by precipitation. In this work, water column ^{7}Be inventories and aerosol ^{7}Be concentrations collected during the 2018 US GEOTRACES Pacific Meridional Transect (PMT; GEOTRACES section GP15) are presented. We use these data together with data from other ocean basins to derive a global relationship between rainfall rate and aerosol bulk deposition velocity. Thus given a global rain product, a means to estimate deposition velocities based on rainfall is provided.

2. Background

The bulk flux for aerosol TEs (F_{TE}) is estimated from the concentration of trace elements in aerosols (C_{TE}) and the bulk deposition velocity (V_b), which includes dry + wet deposition, such that

$$F_{TE} = V_b \times C_{TE} \quad (1)$$

Based on ^{7}Be, V_b can be derived from

Table 1
^{7}Be Data From the PMT (GP15) Cruise: Water Column ^{7}Be Inventories

Station	Lat (°N)	^{7}Be inventory (dpm/m^{2})
4	54.7	23,390
5	53.7	21,520
6	52.0	24,750
8	47.0	25,460
10	42.0	22,580
12	37.0	22,470
14	32.0	22,460
16	27.0	19,980
18	22.0	15,860
19	17.5	21,900
21	11.0	18,240
23	7.5	29,830
25	5.0	28,880
27	2.5	15,550
29	0	4,015
31	−2.5	8,020
33	−5.0	1,730
35	−10.5	16,640
37	−15	21,610
39	−20	23,320

$$V_b = \frac{[^{7}\text{Be flux}]}{(^{7}\text{Be})_{\text{aerosol}}} \quad (2)$$

Furthermore, it has been shown that the integrated rate of decay of ^{7}Be in the upper ocean (i.e., the ^{7}Be inventory in the water column multiplied by the radioactive decay constant for ^{7}Be) is equal to its flux to the ocean by wet and dry deposition (Aaboe et al., 1981; Kadko & Prospero, 2011; Kadko et al., 2015; Kadko et al., 2019). Under steady-state conditions in the absence of upwelling and when particle export of ^{7}Be is negligible (conditions characteristic of most open ocean regions; Kadko & Johns, 2011; Kadko, 2017),

$$V_b = \left(\text{Inventory}^{7}\text{Be} \times \lambda\right) / \left(^{7}\text{Be}\right)_{\text{aerosol}} \quad (3)$$

where λ is the ^{7}Be decay constant (0.013 d^{-1}). This observation provides a key linkage between the atmospheric concentrations of chemical species and their deposition to the oceans; the flux from the atmosphere to the surface ocean of any material having a deposition velocity similar to that of ^{7}Be can be calculated from its atmospheric concentration and the ^{7}Be-derived bulk deposition velocity (Young & Silker, 1980).

This method was tested at the Bermuda Atlantic Time Series (BATS) site in the Sargasso Sea (Kadko et al., 2015), where TE fluxes based on the ^{7}Be method were compared with 24 months of continuous aerosol and rainfall sampling at the Bermuda Institute of Ocean Sciences (BIOS) station on Bermuda. The atmospheric fluxes of total aerosol TEs (Fe, Mn, Co, Ni, Cu, Zn, Cd, and Pb), calculated using the bulk deposition velocity determined from the ^{7}Be data, were comparable (50% to 95%) to fluxes derived from measured wet deposition plus estimated dry deposition (assuming V_d = 1,000 m/day) for samples collected on Bermuda. This method was also tested during the 2015 US Arctic GEOTRACES cruise by comparing ^{7}Be-derived TE fluxes to the measured TE accumulation in recently deposited snow. Given the variability in snow and aerosol TE concentration observed over the expedition and the limited time scale of the observations, agreement between the two methods was reasonable (Kadko et al., 2019).

Because it is associated with submicrometer aerosols, the deposition of aerosol ^{7}Be is dominated by rainfall scavenging, and ^{7}Be deposition rates correlate with the rate of precipitation (e.g., Kadko & Prospero, 2011; Kim et al., 1999; Olsen et al., 1985; Peng et al., 2019; Uematsu et al., 1994; Young & Silker, 1980). The ^{7}Be-derived bulk deposition velocities (equation 3) are plotted against rainfall rate (Figure S1 in the supporting information) for the Arctic (low rainfall region, 1,190 m/day; Kadko et al., 2016, 2019) and for Bermuda

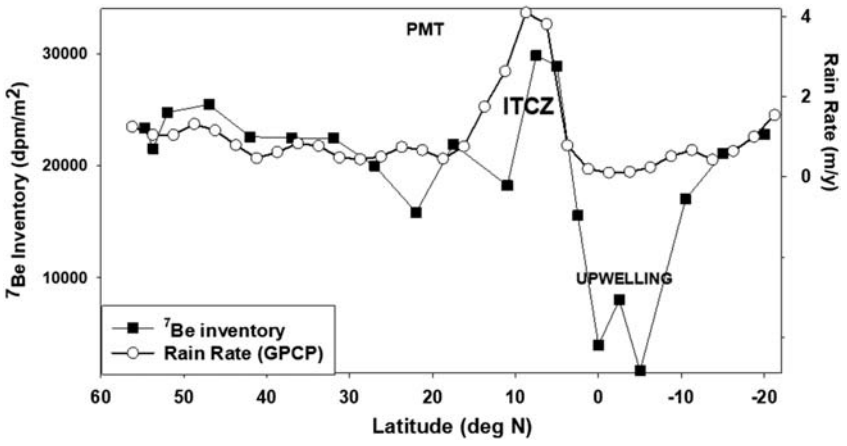

Figure 2. The ^{7}Be inventories (squares) and the weighted average rainfall rate (circles) plotted against latitude for the PMT transect. The locations of the ITCZ and upwelling region are indicated.

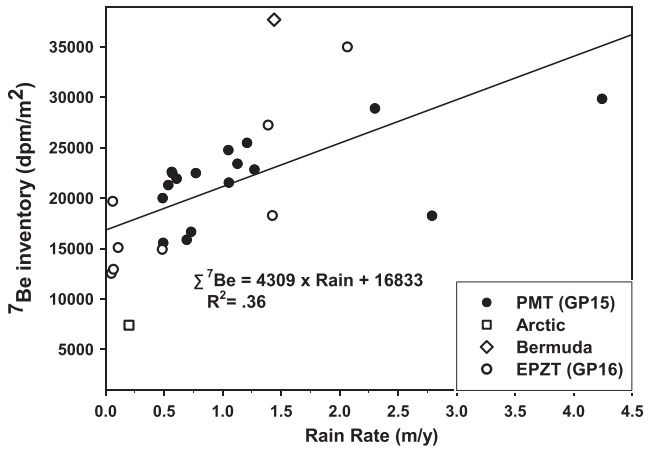

Figure 3. The ^{7}Be inventories plotted against rainfall rate for the PMT cruise (black circles); the EPZT (open circles, Kadko et al., 2020); Bermuda (diamond, Kadko et al., 2015); and the Arctic (square, Kadko et al., 2016, 2019).

(high rainfall region, 2,600 m/day; Kadko et al., 2015). Obviously, a trend cannot be based on only two points, but the zero-rainfall intercept does correspond to the dry deposition velocity of 1,000 m/day generally assumed for dust (e.g., Duce et al., 1991). These results are suggestive of a relationship between V_b and rain rate that will be further explored here.

3. Study Area and Methods

The US GEOTRACES PMT (cruise GP15) was carried out on the R/V Roger Revelle from 25 September to 25 November 2018. The cruise mainly followed a north-to-south track along 152°W between Alaska and Tahiti (Figure 1), designed to examine, among other things, the influence of strong chemical fluxes from the margins, atmospheric dust deposition, oxygen minimum zones, equatorial upwelling, and some of the lowest-nutrient waters in the world ocean in the South Pacific gyre at 20°S. This transect crossed large gradients in rain rate (Figure 1), affording an opportunity to test the V_b and rain rate relationship.

3.1. ^{7}Be Water Column Analysis

Details of sample collection are described in Kadko (2017). Briefly, samples were collected at selected depths by pumping 400–700 L of seawater via a ~4-cm hose into large plastic barrels on deck. From these barrels, the seawater was then pumped through iron-impregnated acrylic fibers at ~10 L/min to extract the ^{7}Be from seawater (Krishnaswami et al., 1972; Lal et al., 1988; Lee et al., 1991). On land, the fibers were dried and then ashed. The ash was subsequently pressed into a pellet (5.8-cm diameter) and placed on a low background germanium gamma detector. The isotope ^{7}Be has a readily identifiable gamma peak at 478 keV. The detector was calibrated for the pellet geometry by adding a commercially prepared mixed solution of known gamma activities to an ashed fiber, pressing the ash into a pellet, and counting the activities to derive a calibration curve. The uncertainty of the extraction efficiency (4%) and the detector efficiency (2%) was in all cases smaller than the statistical counting error and the uncertainty in the blank.

Table 2
^{7}Be Data From the PMT (GP15) Cruise: Aerosol ^{7}Be Activities

Aerosol deployment	Latitude (sample midpoint)	^{7}Be activity (dpm/m^3)
3	54.9	0.0184 ± 0.0066
4	53.3	0.0366 ± 0.0015
1	51.1	0.0622 ± 0.0094
5	49.5	0.1567 ± 0.0054
6	45.75	0.2660 ± 0.0079
7	43.25	0.2935 ± 0.0089
8	39.5	0.1232 ± 0.0053
9	35.75	0.2730 ± 0.0076
10	33.25	0.1818 ± 0.0073
11	29.5	0.2770 ± 0.0083
12	24.5	0.1754 ± 0.0075
13	18.1	0.0975 ± 0.0106
14	14.25	0.0792 ± 0.0084
15	8.8	0.0413 ± 0.0046
16	5.725	0.0984 ± 0.0059
17	3.45	0.1848 ± 0.0079
18	0.415	0.1373 ± 0.0053
19	−3.1	0.1222 ± 0.0105
20	−7.75	0.1492 ± 0.0074
21	−12.75	0.1080 ± 0.0076
22	−17.5	0.1482 ± 0.0066
23	−19.6	0.2147 ± 0.0133

3.2. Aerosol ^{7}Be

Details of the aerosol collection methods are presented in Buck et al. (2019). Briefly, bulk aerosol samples were collected on 12-replicate acid-washed 47-mm Whatman 41(W41) ashless filter discs mounted in Advantec-MFS polypropylene inline filter holders (PP47). When the wind was directed from the bow, air was pumped through the filters using a high-volume aerosol sampler (model 5170V-BL, Tisch Environmental) at approximately 100 L/min through each filter. The sampler was mounted on the forward rail of the 03-deck approximately 16 m above sea level and forward of both the ship's superstructure and exhaust stacks. Each collection period lasted approximately 3 days. For ^{7}Be, Whatman-41 aerosol filters were stacked three-high in a plastic Petri dish and counted by gamma spectroscopy. This configuration was calibrated with a commercially prepared mixed solution of known gamma activities.

3.3. Rainfall Analysis

Rainfall data were derived from the Global Precipitation Climatology Project (GPCP; http://gpcp.umd.edu/). The GPCP monthly product provides a consistent analysis of global precipitation from an integration of various satellite data sets over land and ocean and gauge data from land sites. Detailed methodology and error analyses are presented in Huffman et al. (1997). The rainfall rates used in the following discussions were based on the weighted average at each location, which included the rainfall rate for the month of sampling and the prior 3 months each

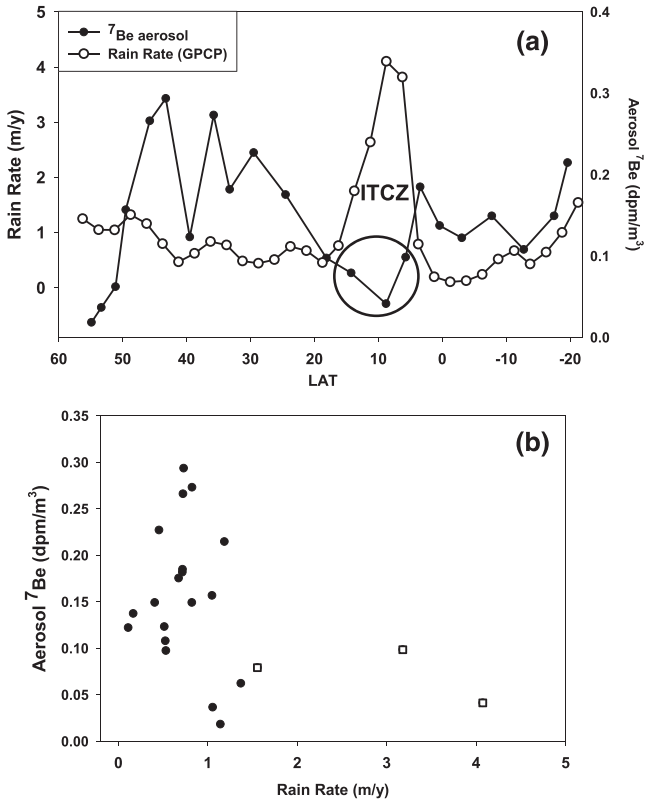

Figure 4. (a) The ^{7}Be aerosol activities (black circles) and weighted average rainfall rate (open circles) plotted against latitude for the PMT cruise track. The location of the ITCZ is indicated and aerosol samples collected within the ITCZ are circled. (b) The ^{7}Be aerosol activities plotted against rain rate. The aerosol samples collected within the ITCZ are indicated (open squares).

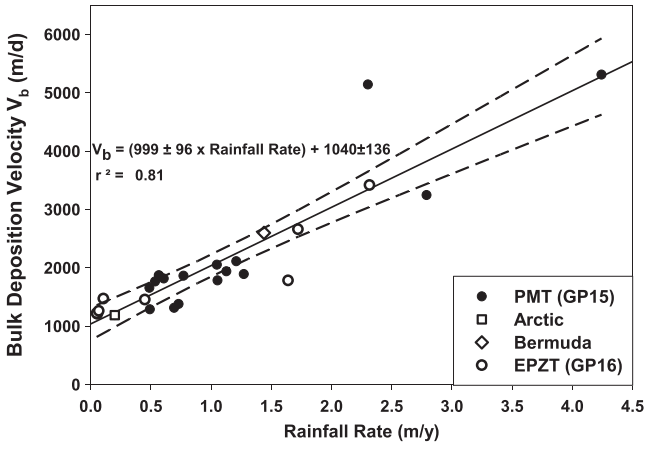

Figure 5. The ^{7}Be-derived V_b plotted against rainfall rate for the PMT cruise (black circles); the EPZT (open circles, Kadko et al., 2020); Bermuda (diamond, Kadko et al., 2015); and the Arctic (square, Kadko et al., 2016, 2019). The upper and lower 95% confidence intervals (dashed lines) around the linear regression trend line are shown.

diminished by an exponential term containing the decay constant of ^{7}Be, that is, weighted against the decay lifetime of ^{7}Be deposited during each month (equation 4).

$$\text{Average rainfall rate} = \Sigma\, RR_i \cdot f_i \exp(-\lambda t_i) / \Sigma\, f_i \exp(-\lambda t_i), \quad (4)$$

where RR_i is the rainfall rate for month (i) taken from the GPCP data set, f_i ($0 \le f_i \le 1$) is the fraction of the month during the month of sampling (e.g., 15 November corresponds to $f = 0.5$), and t_i is the time in days between the sampling date and any previous monthly rain (i).

4. Results and Discussion

Water column ^{7}Be activities are presented in Table S1. The ^{7}Be inventories are shown in Table 1 and plotted against latitude with the weighted average rainfall rates (equation 4) in Figure 2. The gradients in the climatological rainfall rates from Figure 1 are reflected in those of the cruise with the peak in rainfall corresponding to the Intertropical Convergence Zone (ITCZ). Generally, the ^{7}Be inventories follow the trend in rainfall, the exception occurring at the zone of equatorial upwelling. There, the observed ^{7}Be inventory does not reflect atmospheric input, but rather upwelling of deep, ^{7}Be-deficient water. For this reason, the upwelling stations are not included in the subsequent calculations of deposition velocity. The observation of diminished ^{7}Be in upwelling regions has been used to derive upwelling rates (Kadko & Johns, 2011; Haskell et al., 2015; Kadko, 2017). The lower ^{7}Be content and elevated nitrate of these stations (Figure S2) are indicative of upwelling relative to neighboring stations.

The ^{7}Be inventories from this work (PMT) are plotted with those from several earlier studies against rainfall in Figure 3. A general trend of increasing inventory with rainfall rate is observed. These inventories will be combined with the ^{7}Be aerosol concentrations collected with the inventories to derive bulk deposition velocities.

The ^{7}Be aerosol activities from the PMT expedition are shown in Table 2 and plotted against latitude with the weighted average rain rate (equation 4) in Figure 4a. There is no obvious relationship between the ^{7}Be aerosol activities and the rain rate with the exception of aerosols collected within the ITCZ. There the persistent high rainfall maintains a low aerosol ^{7}Be activity (e.g., Feely et al., 1989). This is shown in Figure 4b (a plot of ^{7}Be aerosol concentration against rainfall rate), where the ITCZ samples represent a separate relationship from the other samples. The average ^{7}Be aerosol activity of the three ITCZ samples is 0.073 ± 0.029 dpm/m^{3}, while that for the other 19 samples is 0.157 ± 0.075 dpm/m^{3}.

To derive the bulk deposition velocities (V_b) for the PMT, the ^{7}Be inventories (Table 1) are combined with the aerosol ^{7}Be activities (equation 3; Table 2). The ^{7}Be inventories integrate deposition over the mean life (77 days) of the isotope, and the rainfall rate is based on monthly averages. However, each aerosol sample is collected over a period of only ~3 days, and atmospheric transport is both temporally and spatially sporadic such that variability in aerosol ^{7}Be activity rather than variability in the upper ocean inventory would drive variability in V_b. For this reason, we use the average aerosol ^{7}Be activity rather than the "snapshot" aerosol observations to calculate the bulk deposition velocities. Values of V_b derived in this manner for the PMT cruise are plotted against rainfall rate in

Figure 5. To this are added the values of V_b derived from all the inventories shown in Figure 3, obtained by dividing those data by the appropriate aerosol ^{7}Be concentrations. A high correlation between V_b and rainfall rate is observed across several ocean basins. Scatter observed in the inventory plot (Figure 3) is reduced in the bulk deposition velocity plot (Figure 5) as high inventories (e.g., Bermuda) are driven by high aerosol concentrations, while low inventories (e.g., Arctic) are driven by low aerosol concentrations (refer to equation 3). The resulting relationship is

$$V_b\ (\mathrm{m/day}) = 999 \pm 96 \times \mathrm{RainRate} + 1,\ 040 \pm 136. \quad (5)$$

The y-intercept indicates a dry deposition velocity of 1,040 m/day.

5. Conclusions

In this work, ocean ^{7}Be inventories and aerosol ^{7}Be concentrations collected during the GEOTRACES Pacific Meridional Transect were used with data from other ocean basins to derive a global relationship between rainfall rate (m/yr) and aerosol bulk deposition velocity (m/day), where $V_b = 999 \pm 96 \times$ Rain rate + 1,040 $\pm$ 136 ($R^2 = 0.81$). Future work can further test whether the bulk deposition velocities derived using this relationship, based on aerosol ^{7}Be, can be used to reliably calculate the fluxes of other TEs. This has been tested at Bermuda and the Arctic with good success. With this relationship, the fluxes of soluble aerosol bioactive elements to the surface ocean can be calculated by multiplying the aerosol bulk deposition velocities by the aerosol TE concentrations and solubilities (e.g., Buck et al., 2019; Kadko et al., 2019, 2020). This information is critical for evaluating limitations on phytoplankton growth and the strength of the biological carbon pump and represents an important constraint on ocean biogeochemical models.

Acknowledgments
This work was supported by NSF grants OCE-1736319 to DK, OCE-1756104 to WML, and OCE-1756103 to CSB. Data have been submitted to the Biological and Chemical Oceanography Data Management Office (BCO-DMO) (https://www.bco-dmo.org/dataset/781794 and https://www.bco-dmo.org/dataset/781806) and will appear in future GEOTRACES data products. We thank Drs. Mark Stephens and Chris Marsay for their technical assistance.

References

Aaboe, E., Dion, E. P., & Turekian, K. K. (1981). ^{7}Be in Sargasso Sea and Long Island Sound waters. *Journal of Geophysical Research*, *86*, 3255–3257

Anderson, R. F., Cheng, H., Edwards, R. L., Fleisher, M. Q., Hayes, C. T., Huang, K.-F., et al. (2016). How well can we quantify dust deposition to the ocean? *Philosophical Transactions of the Royal Society A: Mathematical, Physical and Engineering Sciences*, *374*(2081), 20150285. https://doi.org/10.1098/rsta.2015.0285

Baker, A. R., & Jickells, T. D. (2016). Atmospheric deposition of soluble trace elements along the Atlantic Meridional Transect (AMT). *Progress in Oceanography*. https://doi.org/10.1016/j.pocean.2016.10.002

Baker, A. R., Landing, W. M., Bucciarelli, E., Cheize, M., Fietz, S., Hayes, C. T., et al. (2016). Trace element and isotope deposition across the air–sea interface: Progress and research needs. *Philosophical Transactions of the Royal Society A: Mathematical, Physical and Engineering Sciences.*, *374*(2081), 20160190. http://doi.org/10.1098/rsta.2016.0190

Buck, C. S., Aguilar-Islas, A., Marsay, C., Kadko, D., & Landing, W. (2019). Trace element concentrations, elemental ratios, and enrichment factors observed in aerosol samples collected during the US GEOTRACES eastern Pacific Ocean transect (GP16). *Chemical Geology*, *511*, 212–224. https://doi.org/10.1016/j.chemgeo.2019.01.002

Coale, K. H., Johnson, K. S., Fitzwater, S. E., Gordon, R. M., Tanner, S., Chavez, F. P., et al. (1996). A massive phytoplankton bloom induced by an ecosystem-scale iron fertilization experiment in the equatorial Pacific Ocean. *Nature*, *383*, 495–501. https://doi.org/10.1038/3834

Duce, R. A., Liss, P. S., Merrill, J. T., Atlas, E. L., Buat-Menard, P., Hicks, B. B., et al. (1991). The atmospheric input of trace species to the world ocean. *Global Biogeochemical Cycles*, *5*, 193–259. https://doi.org/10.1029/91GB01778

Falkowski, P. (1997). Evolution of the nitrogen cycle and its influence on the biological sequestration of CO_2 in the ocean. *Nature*, *387*, 272–275. https://doi.org/10.1038/387272a0

Falkowski, P. G., Barber, R. T., & Smetacek, V. (1998). Biogeochemical controls and feedbacks on ocean primary production. *Science*, *281*, 200–206.

Feely, H. W., Larsen, R. J., & Sanderson, C. G. (1989). Factors that cause seasonal variations in beryllium-7 concentrations in surface air. *I. Environ. Radioactivity*, *9*, 223–249.

Haskell, W. Z., Kadko, D., Hammond, D. E., Prokopenko, M. G., Berelson, W. M., Knapp, A. N., & Capone, D. (2015). Upwelling velocities and eddy diffusivity from ^{7}Be measurements used to compare vertical nutrient fluxes to export POC flux in the Eastern Tropical South Pacific. *Marine Chemistry*, *168*, 140–150. https://doi.org/10.1016/j.marchem.2014.10.004

Huffman, G. J., Adler, R. F., Arkin, P., Chang, A., Ferraro, R., Gruber, A., et al. (1997). The Global Precipitation Climatology Project (GPCP) combined precipitation dataset. *Bulletin of the American Meteorological Society*, *78*(1), 5–20.

Jickells, T. D., Boyd, P., & Hunter, K. A. (2014). Biogeochemical impacts of dust on the global carbon cycle. In P. Knippertz, & J.-B. W. Struut (Eds.), *Mineral Dust: A Key Player in the Earth System* (pp. 359–384). Amsterdam, Netherlands: Springer. ISBN 978-940178978-3.

Kadko, D. (2017). Upwelling and primary production during the U.S. GEOTRACES East Pacific Zonal Transect. *Global Biogeochem. Cycles*, *31*(2), 218–232. https://doi.org/10.1002/2016GB005554

Kadko, D., Aguilar-Islas, A., Bolt, C., Buck, C. S., Fitzsimmons, J. N., Jensen, L. T., et al. (2019). The residence times of trace elements determined in the surface Arctic Ocean during the 2015 US Arctic GEOTRACES expedition. *Marine Chemistry*, *208*, 56–69. https://doi.org/10.1016/j.marchem.2018.10.011

Kadko, D., Aguilar-Islas, A., Buck, C. S., Fitzsimmons, J. N., Landing, W. M., Shiller, A., et al. (2020). Sources, fluxes and residence times of trace elements measured during the U.S. GEOTRACES East Pacific Zonal Transect. *Marine Chemistry*. https://doi.org/10.1016/j.marchem.2020.103781

Kadko, D., Galfond, B., Landing, W. M., & Shelley, R. U. (2016). Determining the pathways, fate, and flux of atmospherically derived trace elements in the Arctic Ocean/ice system. *Marine Chemistry*, *182*, 38–50. https://doi.org/10.1016/j.marchem.2016.04.006

Kadko, D., & Johns, W. (2011). Inferring upwelling rates in the equatorial Atlantic using ^{7}Be measurements in the upper ocean. *Deep-Sea Research Part I*, *58*, 247–257. https://doi.org/10.1016/j.dsr.2011.03.004

Kadko, D., Landing, W. M., & Shelley, R. U. (2015). A novel tracer technique to quantify the atmospheric flux of trace elements to remote ocean regions. *Journal of Geophysical Research: Oceans*, *119*. https://doi.org/10.1002/2014JC010314

Kadko, D., & Prospero, J. (2011). Deposition of ^{7}Be to Bermuda and the regional ocean: Environmental factors affecting estimates of atmospheric flux to the ocean. *Journal of Geophysical Research*, *116*, C02013. https://doi.org/10.1029/2010JC006629

Kim, G., Alleman, L., & Church, T. (1999). Atmospheric depositional fluxes of trace elements, ^{210}Pb and ^{7}Be into the Sargasso Sea. *Global Biogeochemical Cycles*, *13*, 1183–1192.

Krishnaswami, S., Lal, D., Somayajulu, B. L. K., Dixon, F. S., Stonecipher, S. A., & Craig, H. (1972). Silicon, radium, thorium and lead in seawater: In-situ extraction by synthetic fibre. *Earth and Planetary Science Letters*, *16*, 84–90. https://doi.org/10.1016/0012-821X(72)90240-3

Krishnamurthy, A., Moore, J. K., Mahowald, N., Luo, C., Doney, S. C., Lindsay, K., & Zender, C. S. (2009). Impacts of increasing anthropogenic soluble iron and nitrogen deposition on ocean biogeochemistry. *Global Biogeochemical Cycles*, *23*. https://doi.org/10.1029/2008GB003440

Lal, D., Chung, Y., Platt, T., & Lee, T. (1988). Twin cosmogenic radiotracer studies of phosphorus recycling and chemical fluxes in the upper ocean. *Limnology and Oceanography*, *336*, 1559–1567.

Mahowald, N. M., Baker, A. R., Bergametti, G., Brooks, N., Duce, R. A., Jickells, T. D., et al. (2005). Atmospheric global dust cycle and iron inputs to the ocean. *Global Biogeochem. Cycle*, *19*, GB4025. https://doi.org/10.1029/2004GB002402

Marsay, C. M., Kadko, D., Landing, W. M., Morton, P. L., Summers, B. A., & Buck, C. S. (2018). Concentrations, provenance and flux of aerosol trace elements during US GEOTRACES Western Arctic cruise GN01. *Chemical Geology*, *502*, 1–14.

Martin, J. H., Fitzwater, S. E., & Gordon, R. M. (1990). Iron deficiency limits phytoplankton growth in Antarctic waters. *Global Biogeochem. Cycle*, *4*, 5–12.

Moore, C. M., Mills, M. M., Achterberg, E. P., Geider, R. J., LaRoche, J., Lucas, M. I., et al. (2009). Large-scale distribution of Atlantic nitrogen fixation controlled by iron availability. *Nature Geoscience*, *2*(12), 867–871. https://doi.org/10.1038/ngeo667

Moore, C. M., Mills, M. M., Arrigo, K. R., Berman-Frank, I., Bopp, L., Boyd, P. W., et al. (2013). Processes and patterns of oceanic nutrient limitation. *Nature Geoscience*, *6*(9), 701–710. https://doi.org/10.1038/ngeo1765

Moore, J. K., Doney, S. C., Glover, D. M., & Fung, I. Y. (2002). Iron cycling and nutrient-limitation patterns in surface waters of the World Ocean. *Deep-Sea Research Part II-Topical Studies in Oceanography*, *49*, 463–507.

Morel, F. M. M., Milligan, A. J., & Saito, M. A. (2003). Marine bioinorganic chemistry: The role of trace metals in the oceanic cycles of major nutrients. In H. Elderfield (Ed.), *The oceans and marine geochemistry. Treatise on geochemistry*, (pp. 113–143). Oxford: Elsevier.

Morel, F. M. M., & Price, N. M. (2003). The biogeochemical cycles of trace metals in the oceans. *Science*, *300*(5621), 944–947. https://doi.org/10.1126/science.1083545

Okin, G. S., Baker, A. R., Tegen, I., Mahowald, N. M., Dentener, F. J., Duce, R. A., et al. (2011). Impacts of atmospheric nutrient deposition on marine productivity: Roles of nitrogen, phosphorus, and iron. *Global Biogeochemical Cycles*, *25*(2, n/a). https://doi.org/10.1029/2010GB003858

Olsen, C. R., Larsen, I. L., Lowry, P. D., Cutshall, N. H., & Todd, J. F. (1985). Atmospheric fluxes and marsh-soil inventories of ^{7}Be and ^{210}Pb. *Journal of Geophysical Research*, *90*(10), 487–495.

Peng, A., Liu, G., Jiang, Z., Liu, G., & Liu, M. (2019). Wet depositional fluxes of ^{7}Be and ^{210}Pb and their influencing factors at two characteristic cities of China. *Applied Radiation and Isotopes*, *147*, 21–30. https://doi.org/10.1016/j.apradiso.2019.01.016

Prospero, J. M. (1996). Saharan dust transport over the North Atlantic Ocean and Mediterranean: An overview. In S. Guerzoni, & R. Chester (Eds.), *The impact of desert dust across the Mediterranean* (Vol. 11, pp. 133–151). *Environmental Science and Technology Library*. Dordrecht: Kluwer Academic Publisher. ISBN 978-94-017-3354-0

Prospero, J. M. (2002). The chemical and physical properties of marine aerosols: An introduction. In A. Gianguzza, E. Pelizzetti, & S. Sammartano (Eds.), *Chemistry of marine water and sediments* (pp. 35–82). *Environmental Science*. Berlin, Heidelberg: Springer. https://doi.org/10.1007/978-3-662-04935-8_2

Schanze, J. J., Schmitt, R. W., & Yu, L. L. (2010). The global oceanic freshwater cycle: A state-of-the-art quantification. *Journal of Marine Research*, *68*, 569–595.

Shelley, R. U., Roca-Martí, M., Castrillejo, M., Sanial, V., Masqué, P., Landing, W. M., et al. (2017). Quantification of trace element atmospheric deposition fluxes to the Atlantic Ocean (> 40°N; GEOVIDE, GEOTRACES GA01) during spring 2014. *Deep Sea Research Part I: Oceanographic Research Papers*, *119*, 34–49. https://doi.org/10.1016/j.dsr.2016.11.010

Tagliabue, A., Aumont, O., DeAth, R., Dunne, J. P., Stephanie, D., Galbraith, E., et al. (2015). How well do global ocean biogeochemistry models simulate dissolved iron distributions? *Global Biogeochem. Cycle*, *30*, 149–174. https://doi.org/10.1002/2015GB005289

Tagliabue, A., Bopp, L., & Aumont, O. (2009). Evaluating the importance of atmospheric and sedimentary iron sources to Southern Ocean biogeochemistry. *Geophysical Research Letters*, *36*, L13601. https://doi.org/10.1029/2009GL038914

Uematsu, M., Duce, R. A., & Prospero, J. M. (1994). Atmosphere beryllium-7 concentrations over the Pacific Ocean. *Geophysical Research Letters*, *21*, 561–564.

Volk, T., & Hoffert, M. I. (1985). Ocean carbon pumps: Analysis of relative strengths and efficiencies in ocean-driven atmospheric CO_2 changes. In E. T. Sundquist, & W. S. Broecker (Eds.), *The carbon cycle and atmospheric CO_2: Natural variations Archean to present* (pp. 99–110). Washington, D. C: American Geophysical Union.

Young, J. A., & Silker, W. B. (1980). Aerosol deposition velocities on the Pacific and Atlantic Oceans calculated from ^{7}Be measurements. *Earth and Planetary Science Letters*, *50*, 92–104. https://doi.org/10.1016/0012-821X(80)90121-1